Impaired Glomerular Maturation and Lack of VEGF165b in Denys-Drash Syndrome

Valérie Anne Schumacher,* Stefanie Jeruschke,* Frank Eitner,† Jan Ulrich Becker,‡ Gerald Pitschke,* Yasemin Ince,* Jeffrey H. Miner,§ Ivo Leuschner,‖ Rainer Engers,¶ Anne Schulze Everding,** Monika Bulla,** and Brigitte Royer-Pokora*

**Institute of Human Genetics and Anthropology and ¶Institute of Pathology, Heinrich-Heine-University of Duesseldorf, Duesseldorf, Germany; †Division of Nephrology and Clinical Immunology, University of Aachen, Aachen, Germany; ‡Institute of Pathology and Neuropathology, University Hospital Essen, Essen, Germany; §Renal Division, Departments of Internal Medicine and Cell Biology and Physiology, Washington University School of Medicine, St. Louis, Missouri; ‖Institute of Pediatric Pathology, University of Kiel, Germany; and **Department of Pediatrics, University Children's Hospital of Muenster, Muenster, Germany*

Individuals with Denys-Drash syndrome (DDS) develop diffuse mesangial sclerosis, ultimately leading to renal failure. The disease is caused by mutations that affect the zinc finger structure of the Wilms' tumor protein (WT1), but the mechanisms whereby these mutations result in glomerulosclerosis remain largely obscure. How WT1 regulates genes is likely to be complex, because it has multiple splice forms, binds both DNA and RNA, and associates with spliceosomes. Herein is described that in DDS podocytes, the ratio of both *WT1* +KTS isoforms C to D differs considerably from that of normal child and adult control podocytes and more closely resembles fetal profiles. Aside from the delay in podocyte maturation, DDS glomeruli show swollen endothelial cells, reminiscent of endotheliosis, together with incompletely fused capillary basement membranes; a dramatic decrease in collagen α4(IV) and laminin β2 chains; and the presence of immature or activated mesangial cells that express α-smooth muscle actin. Because appropriate vascular endothelial growth factor A (VEGF-A) expression is known to be essential for the development and maintenance of glomerular architecture and function, this article addresses the question of whether VEGF-A expression is deregulated in DDS. The data presented here show that DDS podocytes express high levels of the proangiogenic isoform *VEGF165*, but completely lack the inhibitory isoform *VEGF165b*. The *VEGF165/VEGF165b* ratio in DDS resembles that of fetal S-shaped bodies, rather than that of normal child or adult control subjects. The alteration in VEGF-A expression presented here may provide a mechanistic insight into the pathogenesis of DDS.

J Am Soc Nephrol 18: 719–729, 2007. doi: 10.1681/ASN.2006020124

Denys-Drash syndrome (DDS) is a rare urogenital disorder that is associated with male pseudohermaphroditism, a high risk for Wilms' tumors, and diffuse mesangial sclerosis, which presents before the age of 2 yr and progresses rapidly to end-stage renal failure (1–3). The disease is mainly caused by heterozygous germline missense mutations in exons 8 and 9 of the Wilms' tumor-1 (*WT1*) gene, encoding zinc finger 2 and 3 of the protein. Despite this knowledge, the mechanisms whereby these mutations result in glomerulosclerosis are poorly understood. WT1 is a zinc finger transcription factor that is expressed throughout urogenital development and continues to be expressed in mature podocytes (4,5). Alternative splicing of the transcript results in four major isoforms, designated A (−/−), B (+/−), C (−/+) and D (+/+) to indicate the presence or absence of exon 5 and KTS, respectively. Isoforms that lack the three amino acids KTS between zinc finger 3 and 4 (−KTS) bind to DNA and are active in transcriptional regulation, whereas KTS-containing variants (+KTS) preferentially bind to RNA and may be involved in RNA processing (6,7). As shown by Hammes *et al.* (8), early kidney development in mice occurs despite the lack of either the +KTS or −KTS splice variants. However, glomerular differentiation and the prevention of glomerulosclerosis require both variants. This is in accordance with observations that were made in individuals with Frasier syndrome, who showed a reduction of +KTS variants as a consequence of intronic *WT1* mutations and subsequently develop glomerulosclerosis in adolescence (9,10).

The crucial role of WT1 in kidney development is further supported by defects that are seen in various mouse models and organ cultures. Depending on *WT1* expression levels,

Received February 6, 2006. Accepted December 20, 2006.

Published online ahead of print. Publication date available at www.jasn.org.

V.A.S.'s current affiliation is the Department of Medicine, Children's Hospital, Boston, Massachusetts. G.P.'s current affiliation is Organon, Clinical Research, Oberschleissheim, Germany. Y.I.'s current affiliation is Institute of Biochemistry and Molecular Biology I, Heinrich-Heine-University of Duesseldorf, Duesseldorf, Germany.

Address correspondence to: Dr. Valérie A. Schumacher, Department of Medicine, Children's Hospital, Boston, MA 02115. Phone: 211-811-2356; Fax: 211-811-2538; E-mail: valerie.schumacher@childrens.harvard.edu

Copyright © 2007 by the American Society of Nephrology

ISSN: 1046-6673/1803-0719

nephrogenesis is impaired completely (11), arrested at the comma-shaped body stage, or delayed (12,13). It is interesting that mice that express a truncated form of WT1 show abnormal glomerular capillary development, suggesting that WT1 may control the expression of growth factors that affect endothelial cells and capillary structure (14). A similar mechanism may also be involved in early kidney development at the time when the metanephric mesenchyme interacts with angioblasts. As was shown recently by Gao *et al.* (15), WT1 regulates the expression of VEGF-A in metanephric mesenchyme, which in turn elicits an as-yet-unidentified signal from the angioblast, that is necessary for branching morphogenesis and nephrogenesis.

VEGF-A also exerts its function later in glomerular development and in the maintenance of the glomerular filtration barrier as shown in mice by Eremina *et al.* (16,17). The most abundant isoform, VEGF165, which in glomeruli is almost exclusively expressed by podocytes, becomes first detectable in S-shaped bodies (18,19) and stimulates endothelial cell migration, proliferation, and differentiation. Recently, a new isoform (VEGF165b) was found to inhibit VEGF165-mediated human umbilical vein endothelial cell proliferation and migration (20), VEGF165-mediated vasodilatation *ex vivo* (20), and angiogenesis *in vivo* (21) and to prevent VEGF165-mediated vascular endothelial growth factor receptor 2 (VEGFR2) phosphorylation and signaling in cultured cells (22). It is interesting that the inhibitory isoform is present in differentiated podocytes but absent in dedifferentiated podocytes (23). This splicing switch suggests that the maturation of podocytes, endothelial cells, and hence glomerular basement membrane (GBM) depends on the ratio of both isoforms.

In this report, we compared the maturation states of podocytes, endothelial cells, GBM, and mesangial cells in DDS kidneys with those of normal fetal, child, and adult control kidneys. Our data suggest that *WT1* mutations in DDS may affect *VEGF165* splicing, which in turn results in an arrest of glomerular maturation and ultimately leads to glomerulosclerosis.

Materials and Methods

Patients and Tissue Samples

Formalin-fixed, paraffin-embedded or snap-frozen specimens from four fetal (estimated gestational age 16 to 27 wk), 10 child, eight adult, and nine DDS kidneys were included in this study. Normal control kidneys from children and adults were obtained from tumor nephrectomy specimens. The diagnosis of DDS was confirmed by histologic examination and by the presence of *WT1* missense mutations. Kidneys from individuals with DDS were obtained at the time of nephrectomy, either because of the presence of a Wilms' tumor or before kidney transplantation at ESRD. The parents of individuals with DDS gave informed consent regarding the study, and kidney tissue was used following the guidelines of the local ethics committee. All tissues that were obtained from individuals with DDS contained at least 50 (usually more than 100) glomeruli for histologic evaluation. Table 1 summarizes the details of the analyzed material.

WT1 Mutation Analysis

Of the nine individuals with DDS, four (NS3, NS8, NS9, and NS10) were previously analyzed for *WT1* mutations by PCR/single-strand conformational polymorphism and direct sequencing (24). Here, we analyzed five additional patients with the same method.

Laser Microdissection and RNA Isolation

Cryosections of 10 μm were stained with hematoxylin under RNase-free conditions, followed by rinses in 70, 80, and 100% ethanol and 100% xylene for 3 min. Human sections were air-dried for 3 min, and glomeruli were laser-microdissected using a PixCell II LCM system (Arcturus, Mountain View, CA) for <1 h per section. Total RNA was extracted with the Absolutely RNA Microprep kit (Stratagene, La Jolla, CA). The numbers of microdissected glomeruli per tissue are given in Table 2.

Real-Time Reverse Transcriptase–PCR

cDNA was synthesized by using the TaqMan Reverse Transcription Reagents (Applied Biosystems, Weiterstadt, Germany). Real-time reverse transcriptase–PCR (RT-PCR) was performed in quadruplicate using cDNA transcribed from 50 ng of total RNA, heat-activated TaqDNA polymerase (HotGold Star; Eurogentec, Seraing, Belgium), WT1 oligonucleotides (Table 3; 300 to 900 nM), and a WT1 fluorescence-labeled probe (FAM; 250 nM; 5′-AGCGATAACCACACAACGC-CCATCC-3′) and run on a TaqMan ABI 7700 Sequence Detection System (PE Biosystems, Weiterstadt, Germany). TaqMan reagents for human 18S rRNA were obtained from Applied Biosystems and served as a housekeeping gene. Cycle conditions for *WT1* were as follows: 2 min at 50°C, 10 min at 95°C, 50 cycles at 95°C for 15 s, and at 60°C for 1 min. Similar amplification efficiencies for all four WT1 PCR were demonstrated by analysis of serial cDNA dilutions that showed a slope value of log input cDNA amount *versus* C_T of <0.1. The ratio of the four WT1 isoforms within one tissue was calculated using the $2^{-\Delta C_T}$ value and was expressed in percentage. The expression of *VEGF165* was determined by real-time RT-PCR using the SYBR Green JumpStart TaqReadyMix (Sigma, Munich, Germany). Cycle conditions were 10 min at 95°C, 40 cycles at 95°C for 30 s, 68°C for 60 s, and 72°C for 60 s. A formula that took into account the different number of WT1-expressing cells (podocytes) per microdissected area of a glomerulus was used:

$$\frac{E_{P1}}{E_{P2}} = \frac{n_1}{n_2} \times \frac{p_2}{p_1} \times \frac{2^{\Delta C_{T2}}}{2^{\Delta C_{T1}}}$$

where E_P is the expression of podocytes in a given tissue, n is the average number of cells per microdissected glomerulus (see Table 4), p is the average number of podocytes per microdissected glomerulus (see Table 4), and ΔC_T is (C_T of WT1) − (C_T of 18S rRNA).

Semiquantitative RT-PCR

cDNA was synthesized using Superscript II reverse transcriptase and hexanucleotide random primers (Invitrogen). PCR was performed as described previously (25) using primers in Table 3 and DMSO for amplification of collagen α1 and α4(IV). Cycle conditions for the PTC200 (Biozym, Hamburg, Germany) machine were hot start at 94°C for 2 min, 40 cycles of 30 s at 94°C, 1 min at 57/59/64/68°C (depending on the gene), 1 min at 72°C, and final extension at 72°C for 10 min. Aliquots of the PCR products were run after 30, 35, and 40 cycles on a 2% agarose gel and visualized by ethidium bromide staining. The volume of the aliquots (5 to 15 μl) was adjusted to allow reliable peak detection and to avoid saturation. The band intensities of RT-PCR products were evaluated using a Phosphoimager FLA 3000 (Raytest, Straubenhardt, Germany) and the AIDA Image Analysis 2.11 (Raytest) software. The relative expression was given after correction for the dilution factor and the applied volume.

Table 1. Patient data, mutation data, and analyses performed in this study[a]

Sample	Age at Nx	Indication	WT1 Mutation	Material	Analyses										
					Real-Time RT-PCR		Semiquantitative RT-PCR					Immunohistochemistry			
					WT1 Isoforms	VEGF-A	Coll IVα1	Coll IVα4	Lam β1	Lam β2	VEGF165/ VEGF165b	WT1	SMA	Coll IVα4	Lam β2
DDS															
NS3	37 mo	DDS	Cys385Arg	P									+		
NS8	38 mo	DDS	Arg394Trp	F, P	D>C						No VEGF165b	+	+	(+)	(+)
NS9	24 mo	DDS	Gly379Cys	F, P							No VEGF165b		+		
NS10	14 mo	DDS	Arg394Trp	F	D>C						No VEGF165b			(+)	(+)
NS18	9 mo	DDS	Arg366His[b]	F	D>C	++	++	−	++	−	No VEGF165b			(+)	(+)
NS19	16 mo	DDS	His373Arg[b]	F	D>C						No VEGF165b			(+)	(+)
NS20	24 mo	DDS	Arg394Trp[b]	P								+	+		
NS21	21 mo	DDS	Cys388Arg[b]	F, P							No VEGF165b	+	+	(+)	(+)
NS22	17 mo	DDS	Arg394Trp[b]	EM											
Fetal															
NEK1	24 wk	Abortion		F	D>C (C)									−(S) ++(C)	−(S) ++(C)
NEK2	16 wk	Abortion		F	D>C (C)	+(S) ++(C)	++(S) +(C)	−(S) ++(C)	++(S) +(C)	−(S) ++(C)	−(S) +(C)				
NEK5	20 wk	Abortion		P								(+)(S) ++(C)	−(S) ++(C)		
NEK6	27 wk	Abortion		P								(+)(S) ++(C)	−(S) ++(C)		
Child															
NAK8	60 mo	WT		F	C>D						VEGF165>VEGF165b			++	++
NAK9	Not known	WT		F		+	+	++	+	++	VEGF165>VEGF165b			++	++
NAK23	84 mo	WT		F							VEGF165>VEGF165b			++	++
NAK27	24 mo	WT		F							VEGF165>VEGF165b				
NAK30	32 mo	WT		F							VEGF165>VEGF165b	++	−		
NAK17	60 mo	WT		P								++	−		
NAK18	24 mo	WT		P								++	−		
NAK19	24 mo	WT		P								++	−		
NAK20	96 mo	WT		P								++	−		
NAK21	24 mo	WT		P								++	−		
Adult															
NAK4	60 to 70 yr	Neoplasm		F	C>D						VEGF165<VEGF165b			++	++
NAK5	60 to 70 yr	Neoplasm		F	C>D						VEGF165<VEGF165b			++	++
NAK6	25 yr	Accident[c]		F							VEGF165<VEGF165b			++	++
NAK7	60 to 70 yr	Neoplasm		F	C>D	+	+	++	+	++	VEGF165<VEGF165b			++	++
NAK10	Not known	Neoplasm		P									−		
NAK13	Not known	Neoplasm		P									−		
NAK14	Not known	Neoplasm		P									−		
NAK15	70 yr	Neoplasm		P								+	−		

[a](C), capillary loop stage; Coll IV, collagen IV; DDS, Denys-Drash syndrome; EM, material for electron microscopy; F, frozen; Lam, laminin; Nx, nephrectomy; P, paraffin-embedded; (S), S-shaped body stage; SMA, smooth muscle actin; VEGF, vascular endothelial growth factor; WT: Wilms' tumor; −, absent; (+), focal positivity; +, positive; ++, prominent positivity.
[b]Mutations found in the present study.
[c]Not suitable as a donor for transplantation because of a bacterial infection.

Table 2. Numbers of laser microdissected glomeruli for RT-PCR[a]

Tissue	No. of Glomeruli
WT1 RT-PCR	
fetal (16 wk) capillary loop ($n = 1$)	60
fetal (24 wk) capillary loop ($n = 1$)	300
child ($n = 1$)	640
adult ($n = 3$)	300 to 400
DDS ($n = 3$)	200 to 360
VEGF, laminin, collagen RT-PCR	
fetal (16 wk) s-shaped body ($n = 1$)	100
fetal (16 wk) capillary loop ($n = 1$)	200
child ($n = 1$)	720
adult ($n = 1$)	300
DDS ($n = 1$)	320

[a]RT-PCR, reverse transcriptase–PCR.

Antibodies and Immunostaining

Immunohistochemistry on formalin-fixed, paraffin-embedded tissues was performed following previously published protocols (26) and on cryosections as described previously (25). Primary antibodies were as follows: For anti-WT1, mAb antibody clone 6F-H2 (DAKO, Hamburg, Germany); for anti-collagen α4(IV), rabbit polyclonal antibody (27); for anti-laminin β2, mouse mAb clone C4 (Hybridoma Bank, Iowa City, IA) (28); and for anti–α-smooth muscle actin (α-SMA), mouse mAb clone 1A4 (DAKO). Morphologic features of the various renal tissues were examined in periodic acid-Schiff–stained sections.

Results

Histopathologic Findings in DDS

DDS glomeruli showed diffuse mesangial sclerosis by light microscopy (Figure 1A). Various stages coexisted in the same specimen with a corticomedullary gradient of involvement, the deepest glomeruli being affected the least: (*1*) Early stages with mild to moderate increase in the mesangial matrix without mesangial cell proliferation; (*2*) fully developed lesion with

Table 3. Primer used for real-time and semiquantitative RT-PCR

Gene	Primer	Location	Sequence 5′-3′	Application
WT1 isoform A (−/−)	WT1–3	Exon 9/10	TGAAGGGCTTTTCACCTGTAT	Real time
	WT1–4	Exon 4/6	CACCTTAAAGGGCCACAGC	
WT1 isoform B (+/−)	WT1–1	Exon 5	AAATGGACAGAAGGGCAGAG	Real time
	WT1–3	Exon 9/10	TGAAGGGCTTTTCACCTGTAT	
WT1 isoform C (−/+)	WT1–2	Exon 9/10	CTGAAGGGCTTTTCACTTGTT	Real time
	WT1–4	Exon 4/6	CACCTTAAAGGGCCACAGC	
WT1 isoform D (+/+)	WT1–1	Exon 5	AAATGGACAGAAGGGCAGAG	Real time
	WT1–2	Exon 9/10	CTGAAGGGCTTTTCACTTGTT	
VEGF165	Forward	Exon 3	CAGCGCAGCTACTGCCATCCAATCGAGA	Real time
	Reverse	Exon 7/8	GCTTGTCACATCTGCAAGTACGTTCGTTTA	
Laminin β1	Forward	Exon 8	CTGGATTCCAGGATGGAAATCA	Semiquantitative
	Reverse	Exon 10	CCAGGTAAACAGCCATGTCAAA	
Laminin β2	Forward	Exon 31	GGCTCTGAAATTGAAACGGGCA	Semiquantitative
	Reverse	Exon 32	GCCGCTGCAGCTTGTCCTGA	
Collagen α1(IV)	Forward	Exon 4	CTACCTGGAACAAAAGGGACAA	Semiquantitative
	Reverse	Exon 9	CCTCTTTCACCTTTCAACAGCA	
Collagen α4(IV)	Forward	Exon 18	GACTCCACCTCTTCCACTTAA	Semiquantitative
	Reverse	Exon 20	GGTTTTCCTGGAGCAGAATCA	
GAPDH	Forward	Exon 8	GGCTCTCCAGAACATCATCCCTGC	Semiquantitative
	Reverse	Exon 8	GGGTGTCGCTGTTGAAGTCAGAGG	
VEGF165/165b	Forward	Exon 7a	GTAAGCTTGTACAAGATCCGCAGACG	Semiquantitative
	Reverse	3′UTR[a]	ATGGATCCGTATCAGTCTTTCCT	

[a]UTR, untranslated region.

Table 4. Determination of WT1-positive cells and total cells/microdissected area of one glomerulus[a]

Tissue	Group	Counted Glomeruli	WT1-Positive Cells (Mean)	Total Cells (Mean)	WT1-Positive Cells/Total Cells (Mean)
NEK1	Fetal (24 wk) c	8	41.3 (±8.5)	60.9 (±13.2)	0.7 (±0.04)
NEK2	Fetal (16 wk) c	9	49.3 (±13.7)	73.0 (±15.5)	0.7 (±0.10)
NEK6	Fetal (27 wk) s	20	26.85 (±7.0)	71.4 (±20.9)	0.4 (±0.09)
NAK8	Child	10	20.8 (±3.9)	41.3 (±7.6)	0.5 (±0.01)
NAK4	Adult	8	15.5 (±3.4)	47.9 (±10.1)	0.3 (±0.01)
NAK5	Adult	10	28.0 (±6.9)	86.7 (±21.0)	0.3 (±0.00)
NS8	DDS	6	22.0 (±7.7)	68.2 (±24.0)	0.3 (±0.02)
NS10	DDS	4	6.8 (±3.1)	20.8 (±9.0)	0.3 (±0.01)
NS18	DDS	10	11.2 (±4.3)	25.3 (±9.7)	0.4 (±0.01)

[a]c, capillary loop stage; s, s-shaped body.

thickening of the basement membranes and massive enlargement of mesangial areas and obliteration of capillary lumens; and (3) advanced stages with the typical nodular, "cannon ball" mesangial sclerosis. These findings are in accordance with those from Habib *et al.* (3,29). Transmission electron microscopy showed massive hyaline deposits with electron-dense strands within sclerosed glomeruli (Figure 2A), and a widespread effacement of podocyte foot processes was found (Figure 2B). Furthermore, endothelial cells were swollen and lacked fenestrae, reminiscent of endotheliosis in eclampsia/preeclampsia (Figure 2B). Finally, incompletely fused basement membranes and fibrillar material between two layers were observed. Together, these findings suggest disturbances in podocyte, endothelial cell, and GBM maturation.

Mutation Analysis and Expression of the WT1 Gene in DDS

We report the mutation analysis of five novel individuals with DDS (NS18, NS19, NS20, NS21, and NS22; Table 1). The other four investigated here (NS3, NS8, NS9, and NS10) were previously described by us (24).

Because missense mutations are thought to act in a dominant negative manner, the presence of a mutant *WT1* transcript/protein is mandatory. By RT-PCR and direct sequencing, it was shown that a mutant transcript is present at similar levels as the wild-type transcript in the analyzed kidneys of patients NS8, NS10, and NS18 (Figure 3 shows transcripts from NS10).

Furthermore, by immunohistochemistry, WT1 was found to be restricted to podocyte precursors during glomerulogenesis

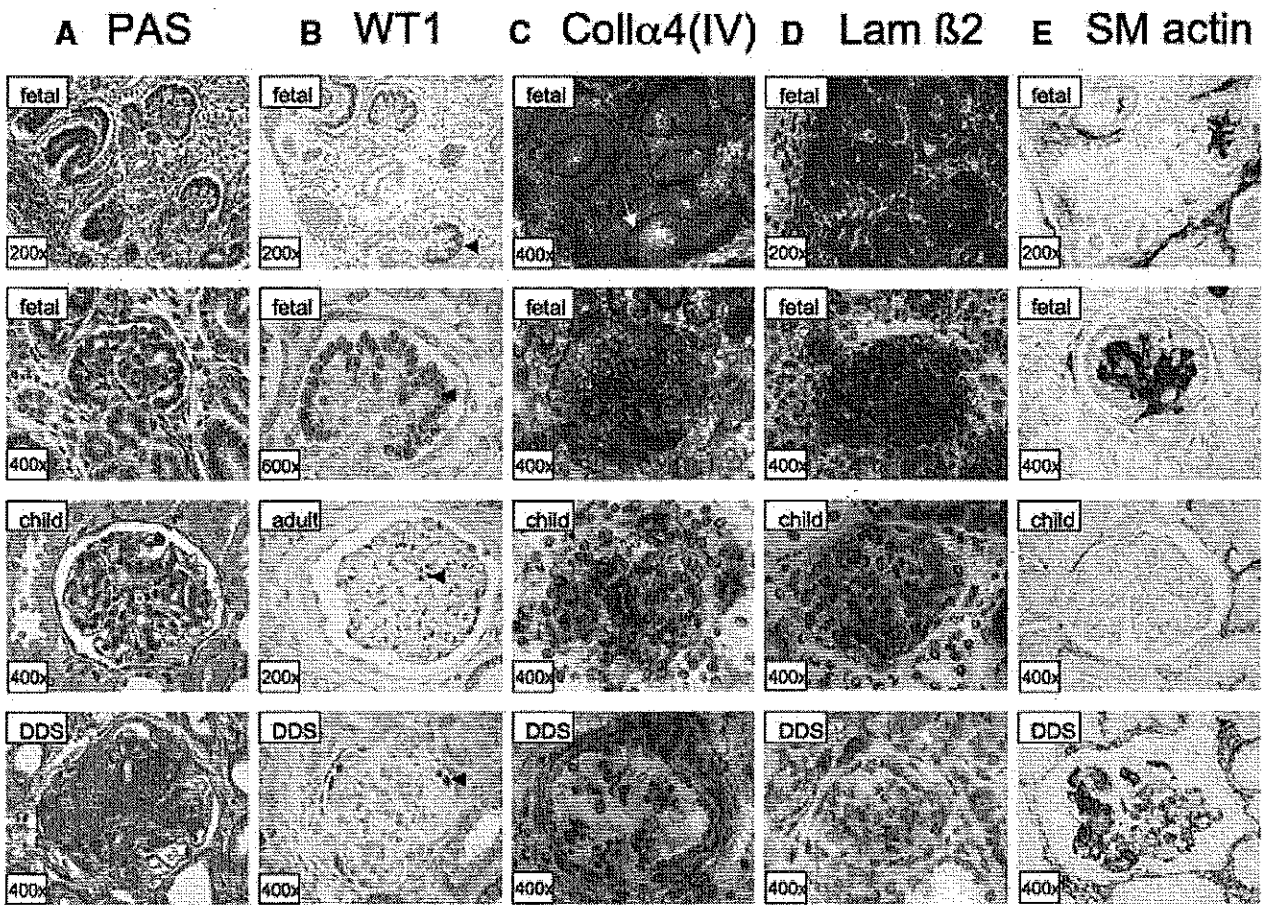

Figure 1. Overview of the periodic acid-Schiff and immunohistochemical staining of fetal, child, adult, and Denys-Drash syndrome (DDS) kidneys. Black arrowheads mark the Wilms' tumor protein (WT1) signal. The white arrow marks the glomerular basement membrane (GBM) stained with collagen α4(IV).

and to podocytes postnatally (Figure 1B), which is in accordance with previous studies (4,5). In DDS, WT1 staining in podocytes was observed in affected glomeruli at all disease stages. However, in advanced stages, a reduced number of WT1-positive nuclei was observed, suggesting a loss of podocytes during progression of the disease (Figure 1B).

Maturation Status of Podocytes in DDS

The molecular marker WT1 was used to analyze the maturation status of podocytes in DDS. Mild to moderately affected glomeruli from four individuals with DDS, glomeruli from three adult control kidneys and one child control kidney, and capillary loop/immature glomeruli from two fetal kidneys (16 and 24 wk of gestation) were laser-microdissected and processed for RT-PCR. Figure 4 demonstrates the ratio of the four main *WT1* mRNA isoforms within a given sample. During development, most obviously, the ratio of isoform C to D changes by increasing continuously: 0.3 in 16-wk-old fetal glomeruli, 0.7 in 24-wk-old fetal glomeruli, 1.7 in glomeruli of a child, and 2.0 (range 1.6 to 2.4) in adults. Glomeruli from individuals with DDS showed a ratio of 0.5 (range 0.3 to 0.7), resembling fetal capillary loop stages. This demonstrates a delay in podocyte maturation in DDS.

Maturation Status of the GBM in DDS

Mild to moderately affected glomeruli from a DDS kidney showed the same distribution of collagen (IV) and laminin β chains as fetal S-shaped bodies, namely high collagen α1(IV) and laminin β1 levels and a lack of collagen α4(IV) and laminin β2 chains (Figure 5). This demonstrates that the developmental switch from collagen α1(IV) to α4(IV) and from laminin β1 to β2 (30) is affected in DDS and that GBM development is arrested at the fetal S-shaped body stage. These data were confirmed in multiple samples by immunohistochemical staining of collagen α4(IV) and laminin β2 (Figure 1; Table 1). Glomerular expression of collagen α4(IV) was first evident within the mesangium and GBM of capillary loop stage glomeruli (Figure 1C). Strong expression persisted in child/adult glomeruli but was significantly reduced in DDS glomeruli. The glomerular deposition of laminin β2 showed a pattern that was similar to that of collagen α4(IV) during the course of glomerular maturation (Figure 1D): Absent in very early glomerular structures,

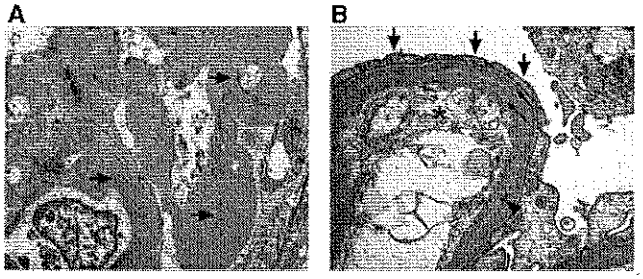

Figure 2. Ultrastructural findings in a patient with DDS (NS22). (A) Sclerosed glomerulus: Massive hyaline deposits with electron-dense fibrin-like structures (arrows). (B) Capillary loop: Complete loss of foot processes (arrows), electron-dense deposits (arrowhead) between the dual layers (thin arrows) of the capillary basement membrane, and endothelial cell with swollen cytoplasm and loss of fenestrations (*). Magnifications: ×2000 in A (transmission electron microscopy); ×15,000 in B (transmission electron microscopy).

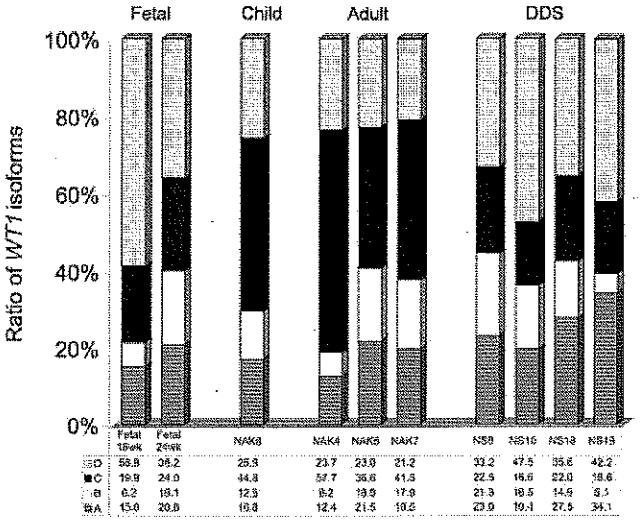

Figure 4. Ratio of the four main *WT1* isoforms A, B, C, and D within one tissue. Glomeruli were laser-microdissected, and expression was measured by real-time reverse transcriptase–PCR (RT-PCR). Glomeruli of fetal kidneys belong to the capillary loop stage. Fetal 16wk, fetal kidney at 16 wk of gestation; Fetal 24wk, fetal kidney at 24 wk of gestation.

strongly positive in the mesangium and GBM of capillary loop stage glomeruli, and persistent expression postnatally. In DDS, the expression of laminin $\beta 2$ was markedly reduced and completely absent in several glomeruli, suggesting a delay in GBM maturation in DDS kidneys.

Maturation Status of the Mesangium in DDS

Immunostaining for α-SMA was performed to evaluate the status of mesangial cells in DDS. As demonstrated in Figure 1E, glomerular α-SMA normally first becomes detectable in the cytoplasm of invading mesangial cells in fetal capillary loop stage glomeruli. In mature human glomeruli, mesangial expression of α-SMA is normally absent, but under disease conditions, α-SMA is detected in activated and/or proliferating mesangial cells (31). In cases of DDS (Figure 1E, bottom), α-SMA is detected within glomeruli, indicating the presence of activated and/or proliferating mesangial cells.

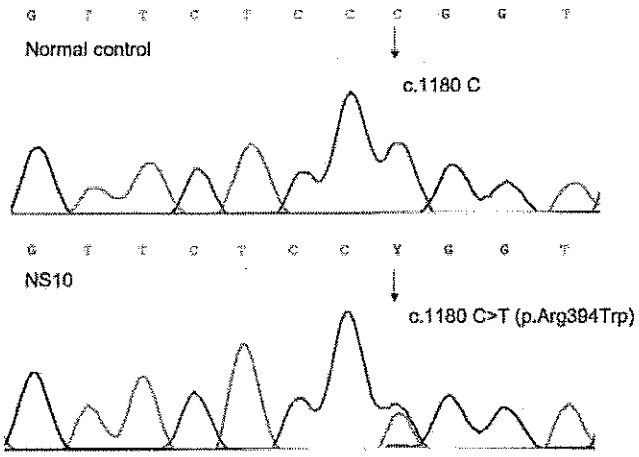

Figure 3. Sequence of *WT1* wild-type and mutant transcripts in patient NS10. (Top) Wild-type WT1 control. (Bottom) Presence of mutant and wild-type transcripts in patient NS10. The position of the mutation (c.1180 C>T) is marked by an arrow.

Altered VEGF165 Splicing in DDS

The data presented here suggest that glomerular maturation in DDS is delayed and affects podocyte, endothelial cell, mesangial cell, and GBM maturation. To address the question of whether this may be caused by disturbed cross-talk between podocytes and endothelial cells, we analyzed VEGF165 as a mediator, which is secreted by podocytes and bound by receptors on endothelial cells. Figure 6A shows the relative amount of the angiogenic stimulatory *VEGF165* mRNA in various tissues after normalization to either 18S rRNA alone or 18S rRNA and the number of podocytes. The amount of *VEGF165* mRNA increases dramatically between the S-shaped body and capillary loop stage in the fetal kidney and decreases in mature glomeruli from a child and an adult. In contrast to our observations in child and adult glomeruli, DDS glomeruli exhibit a major upregulation of VEGF165 expression, which becomes even more marked when the number of podocytes are taken into account.

The ratio of the stimulatory *VEGF165* to the inhibitory *VEGF165b* isoform was determined by semiquantitative RT-PCR. The primers that were used to amplify both forms in a single reaction do not discriminate between the *VEGF165* and *VEGF189* isoforms. However, it was shown previously that *VEGF165* is the most abundant isoform in glomeruli (18,19). During normal development, podocyte maturation is associated with a switch from the stimulatory to the inhibitory isoform (Figure 6B). Therefore, whereas podocytes from fetal S-shaped bodies solely express the stimulatory form, podocytes from the capillary loop stage and onward exhibit increased

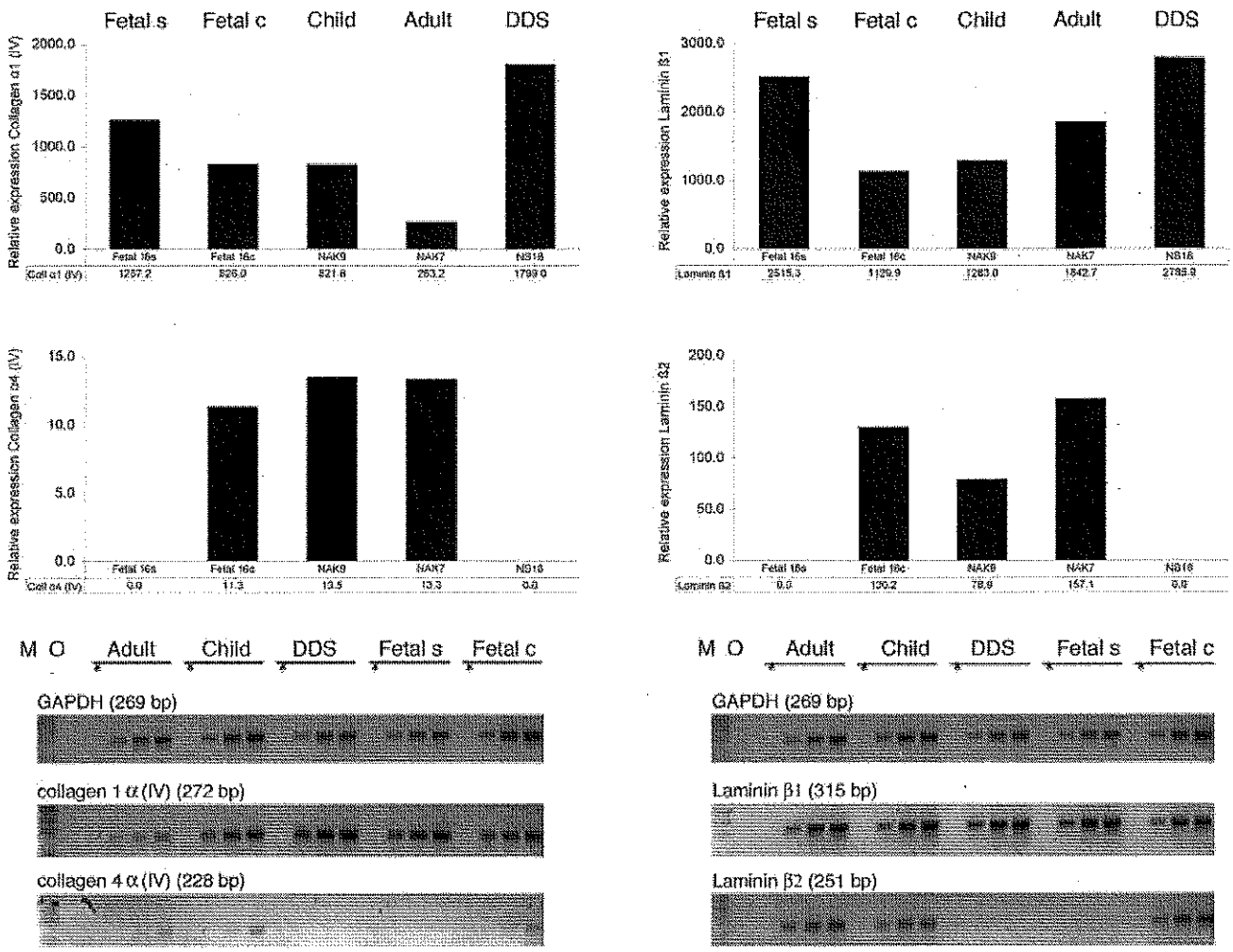

Figure 5. Relative expression of collagen α1(IV) and α4(IV) and laminin β1 and β2 measured by semiquantitative RT-PCR in laser-microdissected S-shaped bodies (s) and capillary loop stage (c) of a 16-wk-old fetal kidney and glomeruli of child/adult and DDS kidneys. It should be noted that the expression values are relative within one isoform and cannot be compared across the isoforms. Expression 0,0, undetectable expression. Aliquots of the PCR products were run on an agarose gel after 30, 35, and 40 cycles. *Control without reverse transcriptase. RT-PCR products were sequenced to confirm that the primers were specific for each isoform chain. GAPDH, glyceraldehyde-3-phosphate dehydrogenase.

expression of *VEGF165b*. In contrast, podocytes from six patients with DDS continue to express the stimulatory isoform *VEGF165* at high levels and fail to express the inhibitory isoform *VEGF165b* (Figure 6C).

Discussion

Our findings suggest that in DDS, glomerular maturation is delayed and VEGF165 splicing is defective. Kidneys from affected patients exhibit complex glomerular disturbances, including an "endotheliosis-like injury of endothelial cells" with the lack/loss of fenestration, incompletely fused basement membranes with a dramatic decrease in collagen α4(IV) and laminin β2 chains, the presence of immature podocytes showing foot process effacement, and the presence of immature or activated mesangial cells.

Abnormal WT1 Expression in DDS Glomeruli

We have demonstrated an overall delay in podocyte maturation in DDS glomeruli, compared with normal child and adult control kidneys. During normal development, isoform D predominates in the fetal capillary loop stage, whereas isoform C becomes more abundant in child and adult glomeruli, suggesting that this latter form may be involved in terminal differentiation processes and in maintaining podocyte function. Remarkably, the ratio of *WT1* isoforms C to D in DDS glomeruli most closely resembles that observed in the fetal kidneys at the capillary loop stage. However, the importance of these observations is unclear, because knockout mice that lack exon 5 corresponding to isoform C do not exhibit an obvious renal phenotype (32).

In addition, DDS glomeruli express mutant transcripts,

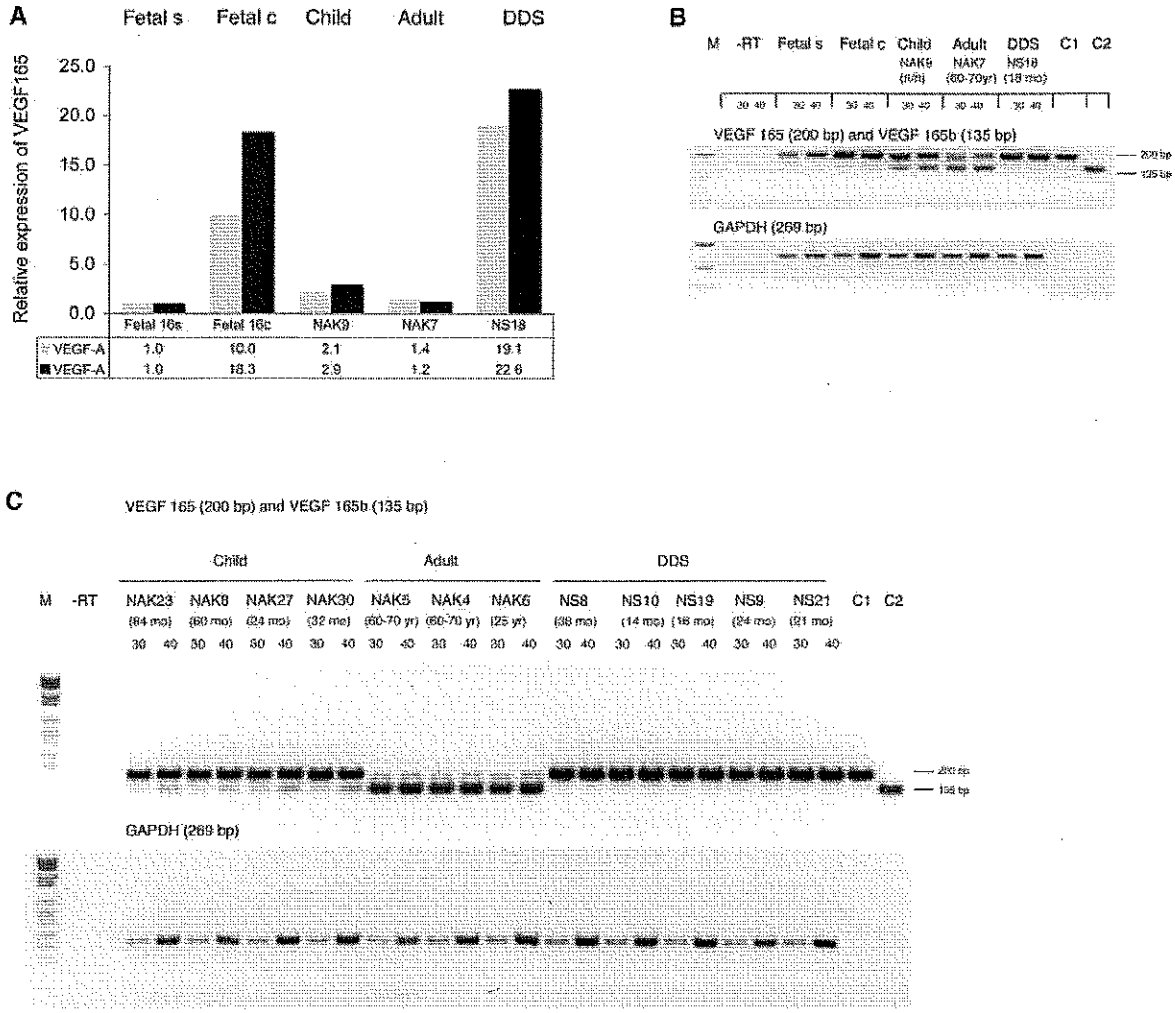

Figure 6. Relative expression of total *VEGF165* and ratio of *VEGF165/VEGF165b* mRNA in laser-microdissected glomeruli. S, S-shaped body; c, capillary loop stage. (A) Relative expression of *VEGF165* determined by real-time RT-PCR and normalized to *18S rRNA* alone (■) or to *18S rRNA* and the podocyte number (▨) (B) Semiquantitative RT-PCR of VEGF165 and VEGF165b. Aliquots of the PCR products from laser-microdissected material were run on an agarose gel after 30 and 40 cycles. −RT, control without reverse transcriptase; Fetal s, laser-microdissected S-shaped bodies from fetal kidney (16 wk of gestation); Fetal c, laser-microdissected capillary loops from fetal kidney (16 wk of gestation); C1, positive control for *VEGF165*; C2, positive control for *VEGF165b*; n/n, not known. (C) Semiquantitative RT-PCR of VEGF165 and VEGF165b. Aliquots of the PCR products from nonmicrodissected material were run on an agarose gel after 30 and 40 cycles. VEGF, vascular endothelial growth factor.

which are thought to act in a dominant negative manner at the protein level, leading to a dramatic loss of functional WT1 protein. Notably, both mouse *in vivo* and organ culture models have shown that glomerulogenesis is a WT1-dependent process (11–14,33). Therefore, abnormal glomerular development in DDS is likely due to loss of wild-type WT1.

Abnormal GBM and Mesangial Cell Maturation in DDS Glomeruli

We further demonstrate that the GBM fails to mature appropriately in DDS. DDS glomeruli express abnormally high levels of collagen α1(IV) and laminin β1, a pattern of aberrant collagen and laminin expression that previously was demonstrated in DDS by Yang *et al.* (34). In addition, DDS glomeruli exhibit dramatic reductions in expression of collagen α4(IV) and laminin β2 chains, factors that normally expressed at high levels in mature glomeruli. Several lines of evidence suggest that collagen α4(IV) and laminin β2 play a critical role in the maintenance of GBM function. *Laminin* β2 knockout mice (35) and individuals with Pierson syndrome as a result of *LAMB2* mutations (which encodes laminin β2) (36) develop proteinuria. Similarly, loss-of-function mutations in *COL4A4* (which encodes collagen α4[IV]) in individuals with Alport syndrome result in severe proteinuria (reviewed in reference [37]).

In our analysis of mesangial cell maturation, we show that DDS glomeruli express α-SMA, a marker for fetal mesangial cells, whereas control child and adult mesangial cells do not

express α-SMA. Together with our previous observations, these results suggest that mesangial cell development is abnormal in DDS glomeruli. However, α-SMA is also expressed in activated mesangial cells after injury, as observed in other diseases (31), alternatively suggesting that mesangial cell activation occurs in DDS glomeruli.

Altered VEGF Expression in DDS Glomeruli

Podocyte–endothelial cell interactions are crucial for the development and maintenance of glomerular architecture and hence the glomerular filtration barrier. Eremina *et al.* (16) elegantly showed that VEGF-A is a key signal that mediates these podocyte–endothelial cell interactions. Indeed, podocyte-specific heterozygosity for VEGF-A results in glomerular maturation defects, glomerulosclerosis (17,16), and swollen endothelial cells (endotheliosis), the latter being part of the renal lesion that is seen in preeclampsia (38). The defects in mice ultimately lead to nephrotic syndrome and ESRD.

There are striking similarities between the phenotype of VEGF-A heterozygous mice and DDS. Together with the previous demonstration that WT1 controls expression of VEGF-A during normal renal development (15), we asked whether loss-of-function mutations in the podocyte-specific *WT1* gene in DDS result in dysregulation of VEGF-A in the podocyte, leading to the DDS phenotype. To address this issue, we focused on the analysis of VEGF165, the predominant VEGF-A isoform in podocytes (18–20).

Our data show that during normal fetal development, angiogenic stimulatory *VEGF165* expression is highest in the capillary loop stage and diminishes thereafter with an isoform switch in favor of the inhibitory *VEGF165b* isoform. *VEGF165b* first becomes detectable at the capillary loop stage and increases continuously, showing the highest expression in adult control glomeruli. It is interesting that the isoform switch of *VEGF165* to *VEGF165b* is paralleled by a change in the ratio from the +KTS *WT1* isoforms C to D, suggesting that the +KTS isoforms may be involved in the alternative splicing of *VEGF165*. In contrast, *VEGF165* expression is elevated in DDS, whereas *VEGF165b* expression is completely abrogated, demonstrating that isoform switching is affected in DDS. Taken together, these results suggest that the complex pathologic changes that are seen in DDS are driven at least in part by a lack of VEGF165b, resulting in disturbed signaling among podocytes, endothelial cells, and mesangial cells. Such a disruption of signaling may be central to the genesis of endotheliosis, GBM, and mesangial cell alterations and may ultimately lead to glomerulosclerosis. Podocytes may respond to these secondary defects by upregulating the stimulatory *VEGF165* isoform, which in turn may enhance glomerular permeability, leading to albuminuria and accumulation of mesangial matrix, as has been postulated for diabetic nephropathy (39).

Our results suggest that *VEGF165* splicing is altered in *WT1* mutated podocytes, resulting in an overall delay in glomerular maturation and glomerulosclerosis. Dysregulated *VEGF165* splicing may reflect a novel pathogenic mechanism that is involved in other diseases. Bates *et al.* (40) showed that inhibitory VEGF isoforms are downregulated, whereas angiogenic stimulatory isoforms are moderately upregulated, in preeclamptic placentas. Complementary studies on diabetic retinopathy demonstrate a switch in splicing from inhibitory to stimulatory isoforms in this disease (41), and in renal cell carcinoma, the inhibitory VEGF165b isoform is downregulated (20). These examples illustrate the importance of maintaining the correct balance between stimulatory and inhibitory VEGF-A isoforms. These observations, together with the similarity of phenotype between DDS and *VEGF-A* heterozygous mice, suggest that at least a portion of the mouse phenotype may be due to an imbalance in the ratio of VEGF isoforms and reduction of VEGF164b expression.

Conclusion

The data presented here illustrate the importance of assessing the ratio of expression between stimulatory and inhibitory VEGF-A isoforms in disease, in contrast to conventional approaches that measured only overall VEGF-A expression. In the future, measuring both stimulatory and inhibitory isoforms may help to resolve conflicting reports concerning the role of VEGF in glomerular disease. We present here the first mechanistic insight into how aberrant expression of *WT1* may affect *VEGF165* splicing and result in glomerulosclerosis in DDS.

Acknowledgments

This work was supported by grants from the Fritz Thyssen Stiftung (V.A.S.), Forschungskommission of the Heinrich-Heine-University of Duesseldorf (V.A.S.), and Heinrich Hertz-Stiftung (V.A.S.). We also acknowledge support from the "Deutsche Nierenstiftung" and the "Stiftung für therapeutische Forschung" from Novartis.

We gratefully acknowledge the interest and participation of all of the families of the affected children. We thank Jordan Kreidberg for many fruitful discussions and great help in reviewing the manuscript, together with Sunny Hartwig and Jacqueline Ho; all of the clinicians and pathologists for providing patient material and clinical data; Peter Graf for clinical data from the child control subjects; Hartwig Kosmehl for providing the paraffin-embedded kidney tissue (NS20); and Dave Bates for the *VEGF165* control cDNA.

Disclosures

None.

References

1. Denys P, Malvaux P, Van Den Berghe H, Tanghe W, Proesmans W: Association of an anatomo-pathological syndrome of male pseudohermaphroditism, Wilms' tumor, parenchymatous nephropathy and XX/XY mosaicism [in French]. *Arch Fr Pediatr* 24: 729–739, 1967
2. Drash A, Sherman F, Hartmann WH, Blizzard RM: A syndrome of pseudohermaphroditism, Wilms' tumor, hypertension, and degenerative renal disease. *J Pediatr* 76: 585–593, 1970
3. Habib R, Loirat C, Gubler MC, Niaudet P, Bensman A, Levy M, Broyer M: The nephropathy associated with male pseudohermaphroditism and Wilms' tumor (Drash syndrome): A distinctive glomerular lesion—Report of 10 cases. *Clin Nephrol* 24: 269–278, 1985
4. Armstrong JF, Pritchard-Jones K, Bickmore WA, Hastie

ND, Bard JB: The expression of the Wilms' tumour gene, WT1, in the developing mammalian embryo. *Mech Dev* 40: 85–97, 1993

5. Mundlos S, Pelletier J, Darveau A, Bachmann M, Winterpacht A, Zabel B: Nuclear localization of the protein encoded by the Wilms' tumor gene WT1 in embryonic and adult tissues. *Development* 119: 1329–1341, 1993
6. Bardeesy N, Pelletier J: Overlapping RNA and DNA binding domains of the WT1 tumor suppressor gene product. *Nucleic Acids Res* 26: 1784–1792, 1998
7. Davies RC, Calvio C, Bratt E, Larsson SH, Lamond AI, Hastie ND: WT1 interacts with the splicing factor U2AF65 in an isoform-dependent manner and can be incorporated into spliceosomes. *Genes Dev* 12: 3217–3225, 1998
8. Hammes A, Guo JK, Lutsch G, Leheste JR, Landrock D, Ziegler U, Gubler MC, Schedl A: Two splice variants of the Wilms' tumor 1 gene have distinct functions during sex determination and nephron formation. *Cell* 106: 319–329, 2001
9. Barbaux S, Niaudet P, Gubler MC, Grunfeld JP, Jaubert F, Kuttenn F, Fekete CN, Souleyreau-Therville N, Thibaud E, Fellous M, McElreavey K: Donor splice-site mutations in WT1 are responsible for Frasier syndrome. *Nat Genet* 17: 467–470, 1997
10. Klamt B, Koziell A, Poulat F, Wieacker P, Scambler P, Berta P, Gessler M: Frasier syndrome is caused by defective alternative splicing of WT1 leading to an altered ratio of WT1 +/−KTS splice isoforms. *Hum Mol Genet* 7: 709–714, 1998
11. Kreidberg JA, Sariola H, Loring JM, Maeda M, Pelletier J, Housman D, Jaenisch R: WT-1 is required for early kidney development. *Cell* 74: 679–691, 1993
12. Moore AW, McInnes L, Kreidberg J, Hastie ND, Schedl A: YAC complementation shows a requirement for Wt1 in the development of epicardium, adrenal gland and throughout nephrogenesis. *Development* 126: 1845–1857, 1999
13. Davies JA, Ladomery M, Hohenstein P, Michael L, Shafe A, Spraggon L, Hastie N: Development of an siRNA-based method for repressing specific genes in renal organ culture and its use to show that the Wt1 tumour suppressor is required for nephron differentiation. *Hum Mol Genet* 13: 235–246, 2004
14. Natoli TA, Liu J, Eremina V, Hodgens K, Li C, Hamano Y, Mundel P, Kalluri R, Miner JH, Quaggin SE, Kreidberg JA: A mutant form of the Wilms' tumor suppressor gene WT1 observed in Denys-Drash syndrome interferes with glomerular capillary development. *J Am Soc Nephrol* 13: 2058–2067, 2002
15. Gao X, Chen X, Taglienti M, Rumballe B, Little MH, Kreidberg JA: Angioblast-mesenchyme induction of early kidney development is mediated by Wt1 and VEGFA. *Development* 132: 5437–5449, 2005
16. Eremina V, Sood M, Haigh J, Nagy A, Lajoie G, Ferrara N, Gerber HP, Kikkawa Y, Miner JH, Quaggin SE: Glomerular-specific alterations of VEGF-A expression lead to distinct congenital and acquired renal diseases. *J Clin Invest* 111: 707–716, 2003
17. Eremina V, Cui S, Gerber H, Ferrara N, Haigh J, Nagy A, Ema M, Rossant J, Jothy S, Miner JH, Quaggin SE: Vascular endothelial growth factor a signaling in the podocyte-endothelial compartment is required for mesangial cell migration and survival. *J Am Soc Nephrol* 17: 724–735, 2006
18. Kretzler M, Schroppel B, Merkle M, Huber S, Mundel P, Horster M, Schlondorff D: Detection of multiple vascular endothelial growth factor splice isoforms in single glomerular podocytes. *Kidney Int Suppl* 67: S159–S161, 1998
19. Robert B, Zhao X, Abrahamson DR: Coexpression of neuropilin-1, Flk1, and VEGF(164) in developing and mature mouse kidney glomeruli. *Am J Physiol Renal Physiol* 279: F275–F282, 2000
20. Bates DO, Cui TG, Doughty JM, Winkler M, Sugiono M, Shields JD, Peat D, Gillatt D, Harper SJ: VEGF165b, an inhibitory splice variant of vascular endothelial growth factor, is down-regulated in renal cell carcinoma. *Cancer Res* 62: 4123–4131, 2002
21. Konopatskaya O, Churchill AJ, Harper SJ, Bates DO, Gardiner TA: VEGF165b, an endogenous C-terminal splice variant of VEGF, inhibits retinal neovascularization in mice. *Mol Vis* 12: 626–632, 2006
22. Woolard J, Wang WY, Bevan HS, Qiu Y, Morbidelli L, Pritchard-Jones RO, Cui TG, Sugiono M, Waine E, Perrin R, Foster R, Digby-Bell J, Shields JD, Whittles CE, Mushens RE, Gillatt DA, Ziche M, Harper SJ, Bates DO: VEGF165b, an inhibitory vascular endothelial growth factor splice variant: Mechanism of action, in vivo effect on angiogenesis and endogenous protein expression. *Cancer Res* 64: 7822–7835, 2004
23. Cui TG, Foster RR, Saleem M, Mathieson PW, Gillatt DA, Bates DO, Harper SJ: Differentiated human podocytes endogenously express an inhibitory isoform of vascular endothelial growth factor (VEGF165b) mRNA and protein. *Am J Physiol Renal Physiol* 286: F767–F773, 2004
24. Schumacher V, Scharer K, Wuhl E, Altrogge H, Bonzel KE, Guschmann M, Neuhaus TJ, Pollastro RM, Kuwertz-Broking E, Bulla M, Tondera AM, Mundel P, Helmchen U, Waldherr R, Weirich A, Royer-Pokora B: Spectrum of early onset nephrotic syndrome associated with WT1 missense mutations. *Kidney Int* 53: 1594–1600, 1998
25. Schumacher V, Schuhen S, Sonner S, Weirich A, Leuschner I, Harms D, Licht J, Roberts S, Royer-Pokora B: Two molecular subgroups of Wilms' tumors with or without WT1 mutations. *Clin Cancer Res* 9: 2005–2014, 2003
26. Eitner F, Ostendorf T, Van Roeyen C, Kitahara M, Li X, Aase K, Grone HJ, Eriksson U, Floege J: Expression of a novel PDGF isoform, PDGF-C, in normal and diseased rat kidney. *J Am Soc Nephrol* 13: 910–917, 2002
27. Miner JH, Sanes JR: Collagen IV alpha 3, alpha 4, and alpha 5 chains in rodent basal laminae: Sequence, distribution, association with laminins, and developmental switches. *J Cell Biol* 127: 879–891, 1994
28. Hunter DD, Shah V, Merlie JP, Sanes JR: A laminin-like adhesive protein concentrated in the synaptic cleft of the neuromuscular junction. *Nature* 338: 229–234, 1989
29. Habib R, Gubler MC, Antignac C, Gagnadoux MF: Diffuse mesangial sclerosis: A congenital glomerulopathy with nephrotic syndrome. *Adv Nephrol Necker Hosp* 22: 43–57, 1993
30. Miner JH: Developmental biology of glomerular basement membrane components. *Curr Opin Nephrol Hypertens* 7: 13–19, 1998
31. Alpers CE, Hudkins KL, Gown AM, Johnson RJ: Enhanced expression of "muscle-specific" actin in glomerulonephritis. *Kidney Int* 41: 1134–1142, 1992
32. Natoli TA, McDonald A, Alberta JA, Taglienti ME, Housman DE, Kreidberg JA: A mammal-specific exon of WT1 is

not required for development or fertility. *Mol Cell Biol* 22: 4433–4438, 2002

33. Guo JK, Menke AL, Gubler MC, Clarke AR, Harrison D, Hammes A, Hastie ND, Schedl A: WT1 is a key regulator of podocyte function: Reduced expression levels cause crescentic glomerulonephritis and mesangial sclerosis. *Hum Mol Genet* 11: 651–659, 2002
34. Yang Y, Zhang SY, Sich M, Beziau A, van den Heuvel LP, Gubler MC: Glomerular extracellular matrix and growth factors in diffuse mesangial sclerosis. *Pediatr Nephrol* 16: 429–438, 2001
35. Noakes PG, Miner JH, Gautam M, Cunningham JM, Sanes JR, Merlie JP: The renal glomerulus of mice lacking s-laminin/laminin beta 2: Nephrosis despite molecular compensation by laminin beta 1. *Nat Genet* 10: 400–406, 1995
36. Zenker M, Aigner T, Wendler O, Tralau T, Muntefering H, Fenski R, Pitz S, Schumacher V, Royer-Pokora B, Wuhl E, Cochat P, Bouvier R, Kraus C, Mark K, Madlon H, Dotsch J, Rascher W, Maruniak-Chudek I, Lennert T, Neumann LM, Reis A: Human laminin beta2 deficiency causes congenital nephrosis with mesangial sclerosis and distinct eye abnormalities. *Hum Mol Genet* 13: 2625–2632, 2004
37. Kashtan CE: Alport syndrome. An inherited disorder of renal, ocular, and cochlear basement membranes. *Medicine (Baltimore)* 78: 338–360, 1999
38. Kincaid-Smith P: The renal lesion of preeclampsia revisited. *Am J Kidney Dis* 17: 144–148, 1991
39. Del Prete D, Anglani F, Ceol M, D'Angelo A, Forino M, Vianello D, Baggio B, Gambaro G: Molecular biology of diabetic glomerulosclerosis. *Nephrol Dial Transplant* 13[Suppl 8]: 20–25, 1998
40. Bates DO, MacMillan PP, Manjaly JG, Qiu Y, Hudson SJ, Bevan HS, Hunter AJ, Soothill PW, Read M, Donaldson LF, Harper SJ: The endogenous anti-angiogenic family of splice variants of VEGF, VEGFxxxb, are down-regulated in pre-eclamptic placentae at term. *Clin Sci (Lond)* 110: 575–585, 2006
41. Perrin RM, Konopatskaya O, Qiu Y, Harper S, Bates DO, Churchill AJ: Diabetic retinopathy is associated with a switch in splicing from anti- to pro-angiogenic isoforms of vascular endothelial growth factor. *Diabetologia* 48: 2422–2427, 2005